

# Theoretical analysis on two-photon absorption spectroscopy in a confined four-level atomic system

Yuanyuan Li (李院院)<sup>1,2\*</sup>, Jintao Bai (白晋涛)<sup>1</sup>, Li Li (李莉)<sup>2</sup>,  
Yanpeng Zhang (张彦鹏)<sup>3</sup>, and Xun Hou (侯洵)<sup>1,4</sup>

<sup>1</sup>Institute of Photonics and Photonic Technology, Key Laboratory of Photoelectronic Technology of Shaanxi Province, Northwest University, Xi'an 710069, China

<sup>2</sup>Department of Physics, Xi'an University of Arts and Science, Xi'an 710065, China

<sup>3</sup>Key Laboratory for Physical Electronics and Devices of the Ministry of Education, Xi'an Jiaotong University, Xi'an 710049, China

<sup>4</sup>State Key Laboratory of Transient Optics and Technology, Xi'an Institute of Optics and Precision Mechanics, Chinese Academy of Sciences, Xi'an 710068, China

\*E-mail: liyynxcn@yahoo.com.cn

Received September 1, 2008

We investigate theoretically two-photon absorption spectroscopy modified by a control field in a confined Y-type four-level system. Dicke-narrowing effect occurs both in two-photon absorption lines and the dips of transparency against two-photon absorption due to enhanced contribution of slow atoms. We also find that the suppression and the enhancement of two-photon absorption can be modified by changing the strength of the control field and the detuning of three laser fields. This control of two-photon absorption may have some applications in information processing and optical devices.

OCIS codes: 300.6320, 020.3690.

doi: 10.3788/COL20090707.0640.

Dicke-narrowing is a phenomenon that dramatically reduces the Doppler width of spectral lines due to frequent velocity-changing collisions. Similar phenomenon occurs for electromagnetically induced transparency (EIT) resonances, and facilitates very narrow spectral features in room temperature vapor<sup>[1]</sup>. As a thin vapor is confined in small size cells, the properties of the spectroscopy can be considerably different from those of large ones if the cell dimensions are small compared to the mean free path of the atoms in the vapor. In this case, the atomic sample becomes anisotropic since atoms flying parallel to the windows interacting with the light much longer than those flying perpendicular to the windows. Such an anisotropy is responsible for the observation of sub-Doppler features in the spectrum<sup>[2,3]</sup>. This type of spectroscopy can be a suitable tool for probing the effective velocity distribution arising from the atomic desorption processes<sup>[3]</sup>, atom-wall interactions<sup>[4-6]</sup>, dark resonances, and EIT<sup>[3-8]</sup> in a confined system. Dicke-narrowing spectroscopy can be extended to two-photon situation, in which absorption lines are dramatically modified by the detuning and the strength of the pump field as well as the thickness of the cell<sup>[9]</sup>. Two-photon absorption in a confined system can also be modified by a control field, in which we will discuss Dicke-narrowing lines and the dips of transparency against two-photon absorption, the suppression, and the enhancement of two-photon absorption. This control of two-photon absorption in a confined system is feasible in experiment, which may have some possible applications such as two-photon lasing and pulse propagation.

We consider atoms confined in a thin vapor cell of thickness  $L$ . Figure 1(a) presents the energy level diagram of the atoms, where  $\Omega_1$ ,  $\Omega_2$ , and  $\Omega_3$  are the tran-

sition frequencies of  $|0\rangle - |1\rangle$ ,  $|1\rangle - |2\rangle$ , and  $|1\rangle - |3\rangle$ , respectively. Two weak laser fields  $\varepsilon_1$  and  $\varepsilon_2$  are applied on the transition of  $|0\rangle - |1\rangle$  and  $|1\rangle - |2\rangle$ , and a control field  $\varepsilon_3$  in arbitrary intensity on the transition of  $|1\rangle - |3\rangle$  respectively. The frequency and the detuning of the field  $\varepsilon_i$  are  $\omega_i$  and  $\Delta_i = \Omega_i - \omega_i$  ( $i = 1, 2, 3$ ), respectively. Signal can be obtained by detecting the absorption of the probe field  $\varepsilon_1$  versus the Raman detuning  $\Delta = \Delta_1 + \Delta_2$ .

The atomic motions are determined by the following coupling equations

$$\begin{aligned} \partial\sigma_{10}/\partial t = & -\Lambda_{10}\sigma_{10} + ig_1(\sigma_{00} - \sigma_{11}) \\ & + ig_2\sigma_{20} + ig_3\sigma_{30}, \end{aligned} \quad (1a)$$

$$\partial\sigma_{20}/\partial t = -\Lambda_{20}\sigma_{20} + ig_2\sigma_{10} - ig_1\sigma_{21}, \quad (1b)$$

$$\partial\sigma_{30}/\partial t = -\Lambda_{30}\sigma_{30} + ig_3\sigma_{10} - ig_1\sigma_{31}, \quad (1c)$$

where the Doppler-shifted detunings are defined as  $\Lambda_{10} = \Gamma_{10} + i(k_1v + \Delta_1)$ ,  $\Lambda_{20} = \Gamma_{20} + i(k_1v + k_2v + \Delta_1 + \Delta_2)$ ,  $\Lambda_{30} = \Gamma_{30} + i(k_1v + k_3v + \Delta_1 + \Delta_3)$  with  $\Gamma_{ij} = \Gamma_{ji} = (\Gamma_i + \Gamma_j)/2$ , which is the decay rate from level  $|i\rangle$  to  $|j\rangle$  ( $i, j = 0, 1, 2, 3$ , and  $i \neq j$ ),  $g_i$  and  $k_i$  are the Rabi frequency and the wave vector of the field  $\varepsilon_i$  ( $i = 1, 2, 3$ ), respectively.

In a thin vapor cell of thickness  $L$ , the absorption of the probe field is given by<sup>[8]</sup>

$$\begin{aligned} \langle A \rangle = & 1 - \exp \left( -N\mu_{10}k_1/\varepsilon_0\varepsilon_1 \int_{-\infty}^{\infty} \int_0^L W(v) \right. \\ & \left. \times \text{Im}[\Theta(v)\sigma_{10}^+ + \Theta(-v)\sigma_{10}^-] dv dz \right), \end{aligned} \quad (2)$$

where  $N$ ,  $\mu_{10}$ , and  $\varepsilon_0$  are the density of atoms in the vapor, the dipole matrix element, and the vacuum permittivity, respectively,  $z$  is the distance perpendicular

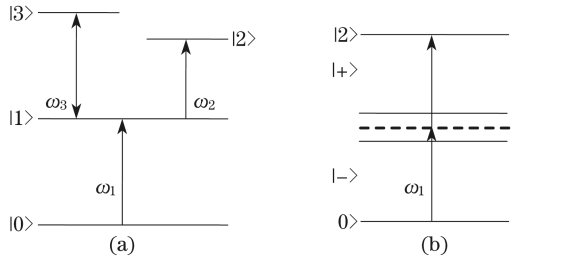


Fig. 1. (a) Energy level diagram and (b) dressed-state picture of Y-type four-level system.

to the cell window, the atomic thermal motion is assumed to obey the Maxwell distribution  $W(v) = (u\sqrt{\pi})^{-1} \exp(-v^2/u^2)$  with  $u$  being the probable velocity,  $\Theta(v)$  and  $\Theta(-v)$  are Heaviside functions,  $\sigma_{10}^+$  and  $\sigma_{10}^-$  are the density matrix elements for  $v > 0$  and  $v < 0$ , respectively.

The steady state solution of Eq. (1) is not useful in the present case because the atoms contributing to the coherence resonance are essentially in transient regime of interaction. In consequence, the matrix  $\sigma_{10}(t)$  as a function of the interaction time elapsed after the atom left the cell window should be obtained<sup>[3]</sup>. We first get a Laplace transformed solution of  $\sigma_{10}$  as

$$\begin{aligned} \mathcal{L}[\sigma_{10}] = & ig_1(s + \Lambda_{20})(s + \Lambda_{30}) / \\ & s[(s + \Lambda_{10})(s + \Lambda_{20})(s + \Lambda_{30}) \\ & + g_2^2(s + \Lambda_{30}) + g_3^2(s + \Lambda_{20})], \end{aligned} \quad (3)$$

where  $s$  is the Laplace variable,  $\sigma_{00} \approx 1$ ,  $\sigma_{11} = \sigma_{22} = \sigma_{33} = 0$ , and  $\sigma_{i0}(t=0) = 0$  ( $i = 1, 2, 3$ ),  $\sigma_{21} = \sigma_{31} = 0$  are assumed to be satisfied.

Next, we write the solution of  $\sigma_{10}(t)$  by applying the inverse-Laplace transform to Eq. (3), which is given by

$$\sigma_{10}(t) = ig_1 \left[ D_0 + \sum_{j=1}^3 D_j \exp(-\lambda_j t) \right], \quad (4)$$

where  $D_0 = \Lambda_{20}\Lambda_{30}/(\lambda_1\lambda_2\lambda_3)$ ,  $D_j = -(\lambda_j - \Lambda_{20})(\lambda_j - \Lambda_{30})/[\lambda_j(\lambda_j - \lambda_2)(\lambda_j - \lambda_3)]$ , and  $\lambda_j$  ( $j = 1, 2, 3$ ) is the root of  $s$  for the denominator in Eq. (5) equal to zero, we do not write them out here since they are very tedious.

Laser-atom interaction time in a thin vapor cell is related to  $z$  through  $t = z/v$  for  $v > 0$  and  $t = (z-L)/v$  for  $v < 0$ , for which we assume that atoms get de-excited at a collision with the wall, and are in the ground states at the instant that they leave the wall after a collision. Substituting Eq. (4) into Eq. (2) and changing the integrate orders of  $v$  and  $z$ , we then have

$$\langle A \rangle = 1 - \exp \left( -N\mu_{10}^2/\varepsilon_0\hbar \int_{-\infty}^{\infty} k_1|v|W(v)dv \text{Im}S \right), \quad (5)$$

where  $S = iD_0L + i\sum D_j|v|/\lambda_j - i\sum D_j|v|/\lambda_j \exp(-\lambda_j L/|v|)$ .

The first term in Eq. (5) represents a Gaussian profile with a full halfwidth  $\delta\omega_D = 2\sqrt{\ln 2}k_1u$  as it is in a macroscopic cell. The second term originates in the buildup of the atomic response to the driving fields, and it illustrates the integration of all possible interaction inside the medium. The third term reflects the finiteness of

the interaction time of  $L/v$ , which is limited by the film thickness<sup>[7-12]</sup>. Thus the second and the third terms are responsible for the transient behavior of atoms in a confined system, which induce Dicke-narrowing structure lines.

One candidate for our numerical calculation is  $^{87}\text{Rb}$  with  $5S_{1/2}$  ( $F = 2$ ),  $5P_{3/2}$ ,  $5D_{3/2}$  and  $5D_{5/2}$ , corresponding to states  $|0\rangle$ ,  $|1\rangle$ ,  $|2\rangle$ , and  $|3\rangle$ , respectively. Transitions of  $|0\rangle \rightarrow |1\rangle$ ,  $|1\rangle \rightarrow |2\rangle$ , and  $|1\rangle \rightarrow |3\rangle$  are at 780 nm, 776.16 nm, and 775.98 nm, respectively. Other selected values are  $L = \lambda/2$ ,  $\Gamma_1 = 2\pi \times 5.9$  MHz,  $\Gamma_2 = \Gamma_3 = 2\pi \times 0.97$  MHz,  $g_2 = 0.03\Gamma_1$ ,  $N = 5.2 \times 10^{12}/\text{cm}^3$ , and  $u = 270$  m/s (assuming the vapor is heated to 180°C). All detunings are in the units of  $\Gamma_1$ .

One-peak Dicke-narrowing lines always occur for a relatively weak control field and the shape is similar to the situation of two-photon lines without a control field [Fig. 2(a)]. As the strength of the control field increases, the intermediate state can be coupled by the control field with another state, i.e., the energy level  $|1\rangle$  is dressed by the coupling field  $\varepsilon_3$  to two intermediate levels  $|+\rangle$  and  $|-\rangle$  [Fig. 1(b)]. The absorption can be viewed as interference effect taking place through two intermediate states. The minimum of absorption is determined by the behavior of interference between two channels  $|0\rangle \rightarrow |+\rangle \rightarrow |2\rangle$  and  $|0\rangle \rightarrow |-\rangle \rightarrow |2\rangle$ <sup>[13]</sup>. Thus two-peak lines of two-photon absorption occur at  $\Delta \approx \Delta_2 - \Delta_3$  [Fig. 2(b)] and the narrow dips, which represents the transparency against two-photon absorption, is mainly from the enhanced contribution of slow atoms in a dark state in a thin cell.

It should also be noted that the control field can either suppress or enhance two-photon absorption in a confined system as shown in Fig. 3. As  $\Delta_1$  and  $\Delta_2$  are tuned to zero, two-photon absorption can be dramatically suppressed [Fig. 3(a)]. In this case, the absorption minimum is dependent on the strength of the control field as EIT condition of  $\Delta_1 = \Delta_2 = -\Delta_3$  is satisfied, where perfect transparency against two-photon absorption can be achieved as a relatively larger  $g_3$  applying to the system. Figure 3(c) shows that the absorption can be totally enhanced for a far detuning of  $g_1$  and  $g_2$  as a control field applying to the system. Semi-suppression and enhancement of two-photon absorption corresponding to the different detuning of  $\Delta_3$  and the strength of the control field are shown in Fig. 3(b). These three cases are determined by the interference effect of two channels of  $|0\rangle \rightarrow |+\rangle \rightarrow |2\rangle$  and  $|0\rangle \rightarrow |-\rangle \rightarrow |2\rangle$ . It could be in phase, in dephase or in semi-dephase corresponding

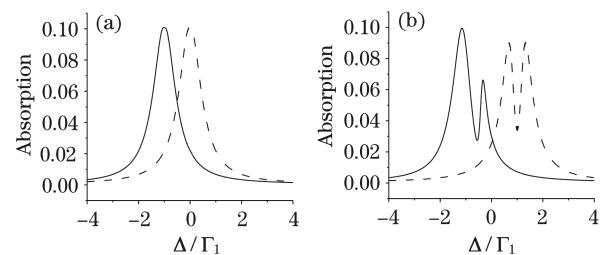


Fig. 2. Absorption lines versus the Raman detuning  $\Delta$  (in  $\Gamma_1$  units). (a)  $\Delta_2 = \Delta_3 = 0$ ,  $g_3 = 0$  (dashed line) and  $\Delta_2 = -\Gamma_1$ ,  $\Delta_3 = 0$ ,  $g_3 = 0.03\Gamma_1$  (solid line); (b)  $\Delta_2 = \Gamma_1$ ,  $\Delta_3 = 0$ ,  $g_3 = 0.3\Gamma_1$  (dashed line) and  $\Delta_2 = -\Gamma_1$ ,  $\Delta_3 = -0.5\Gamma_1$ ,  $g_3 = 0.3\Gamma_1$  (solid line).

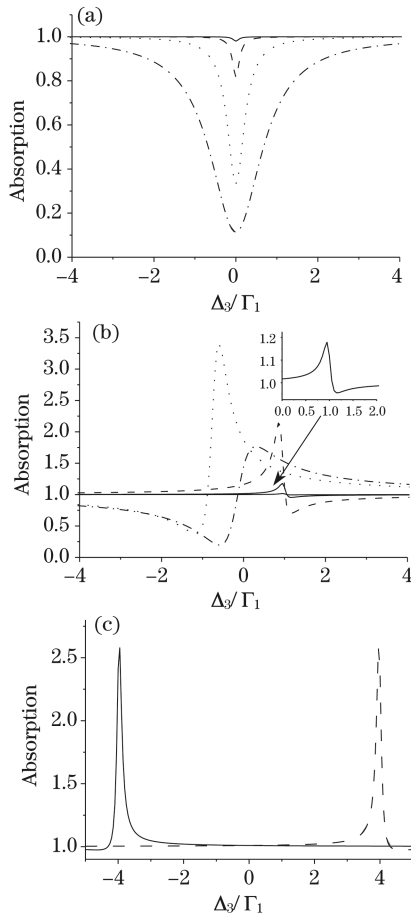


Fig. 3. Absorption versus  $\Delta_3$  (in  $\Gamma_1$  units). (a)  $g_3 = 0.03\Gamma_1$  (solid line),  $g_3 = 0.1\Gamma_1$  (dashed line),  $g_3 = 0.3\Gamma_1$  (dotted line), and  $g_3 = 0.6\Gamma_1$  (dash dot line), other parameters are  $\Delta_1 = \Delta_2 = 0$ ; (b)  $g_3 = 0.1\Gamma_1$  (solid line),  $g_3 = 0.3\Gamma_1$  (dashed line), and  $g_3 = 0.6\Gamma_1$  (dotted and dash dot lines),  $\Delta_1 = \Delta_2 = -\Gamma_1$  (solid, dashed, and dotted lines) and  $\Delta_1 = \Delta_2 = \Gamma_1/2$  (dash dot line); (c)  $\Delta_1 = \Delta_2 = 4\Gamma_1$  (solid line) and  $\Delta_1 = \Delta_2 = -4\Gamma_1$  (dashed line), other parameters are  $g_3 = 0.3\Gamma_1$ . Signal with  $g_3 = 0$  is normalized to be 1.

to enhancement, suppression or semi-suppression, and enhancement, respectively.

We further point out that, such a confined atomic system is different from the cold atomic system. The cold atoms are free Doppler broadening and allow much longer interaction time with the laser fields compared with the case of thermal atomic vapor. The cell can be treated as a macroscopic cell and the typical size of the cold cloud can be in millimeter scale. The experimental setup is expensive and complicated. In a simple confined atomic system, a cell with its thickness typically less than  $10\ \mu\text{m}$  is usually fabricated. Thus the steady state solution is no use in this case and we must consider transient effect of atom-laser interaction. The atom-laser radiation interaction time governed by wall-to-wall trajectories is anisotropic and the contribution of atoms with slow normal velocity is enhanced due to their longer interaction time with the laser field. Under normal incidence irradiation, the resonance of these atoms, flying nearly parallel to the wall and yielding a stronger contribution to the signal, for their relative longer atom-light interaction time. Thus Dicke-narrowing structure of absorption lines is manifest in a Doppler-free configuration. Slow atoms, having a long time of interaction, contribute to the coher-

ent signal through narrow resonances while faster atoms essentially contribute to the wings of the coherent signal. Although slow atoms are rare, their contribution at line center is of comparable importance to that of more abundant fast atoms<sup>[3]</sup>. Moreover, it is narrower contribution of slow atoms that dominates the dips of transparency against two-photon absorption.

In conclusion, we investigate two-photon absorption spectroscopy modified by a control field in a confined system. Similar to a macroscopic cell, the medium can be made transparent against two-photon absorption in a thin cell. Two-photon absorption can be suppressed or enhanced by choosing different detuning of three laser fields and the strength of the control field. Due to the enhanced contribution of slow atoms, very narrow two-photon absorptive lines, EIT dips are obtained in such a confined system. Instead of expensive cold atom technology, it may give an easy way to implement optical information processing. We also suggest that two-photon spectroscopy in a confined system could be a suitable tool for probing the effective velocity distribution in the thin cell arising from the atomic desorption processes. Other interesting phenomenon such as velocity or temperature jumps on a surface or laser induced desorption, transmission or multi-wave-mixing enhancement could also possibly be approached with this technique<sup>[3,14,15]</sup>.

This work was supported by the National Natural Science Foundation of China (No. 10874139) and the Major Program of Science Foundation of Xi'an University of Arts and Science.

References

1. M. Shuker, O. Firstberg, R. Pugatch, A. Ben-Kish, A. Ron, and N. Davidson, *Phys. Rev. A* **76**, 023813 (2007).
2. D. Sarkisyan, D. Bloch, A. Papoyan, and M. Ducloy, *Opt. Commun.* **200**, 201 (2001).
3. H. Failache, L. Lenci, A. Lezama, D. Bloch, and M. Ducloy, *Phys. Rev. A* **76**, 053826 (2007).
4. H. Failache, S. Saltiel, M. Fichet, D. Bloch, and M. Ducloy, *Phys. Rev. Lett.* **83**, 5467 (1999).
5. H. Failache, S. Saltiel, A. Fischer, D. Bloch, and M. Ducloy, *Phys. Rev. Lett.* **88**, 243603 (2002).
6. I. Hamdi, P. Todorov, A. Yaroviski, G. Dutier, I. Maurin, S. Saltiel, Y. Li, A. Lezama, T. Varzhapetyan, D. Sarkisyan, M.-P. Gorza, M. Fichet, D. Bloch, and M. Ducloy, *Laser Phys.* **15**, 987 (2005).
7. Y. Li, X. Hou, J. Bai, J. Yan, C. Gan, and Y. Zhang, *Chin. Phys.* **17**, 2885 (2008).
8. Y. Li, J. Bai, L. Li, W. Zhang, C. Li, Z. Nie, C. Gan, and Y. Zhang, *Chin. Phys. Lett.* **25**, 3238 (2008).
9. Y. Li, J. Bai, G. Zhang, Y. Zhou, Y. Zhang, and C. Gan, *Acta. Phys. Sin.* (in Chinese) **55**, 6293 (2006).
10. Y. Li, Y. Zhang, and C. Gan, *Chin. Opt. Lett.* **3**, 672 (2005).
11. Y. Li, G. Zhang, and Y. Zhou, *Chin. Phys.* **15**, 985 (2006).
12. Y. Li, X. Hou, J. Bai, J. Yan, C. Gan, and Y. Zhang, *Acta Opt. Sin.* (in Chinese) **28**, 1623 (2008).
13. G. S. Agarwal and W. Harshawardhan, *Phys. Rev. Lett.* **77**, 1039 (1996).
14. G. Xiao, X. Yao, X. Ji, J. Zhou, Z. Bao, and Y. Huang, *Chin. Opt. Lett.* **6**, 791 (2008).
15. C. Zuo, Y. Du, T. Jiang, Z. Nie, Y. Zhang, H. Zheng, C. Gan, W. Zhang, and K. Lu, *Chin. Opt. Lett.* **6**, 685 (2008).